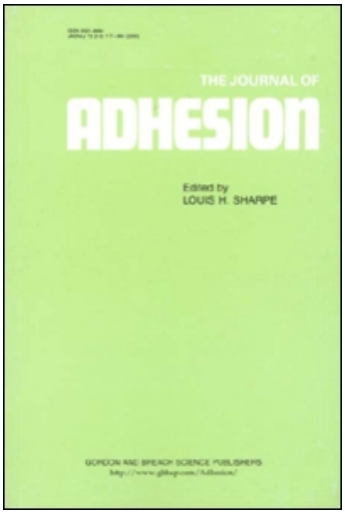

The Journal of Adhesion
Publication details, including instructions for authors and subscription information:
http://www.informaworld.com/smpp/title~content=t713453635

The Durability of Adhesively-bonded Ti-6Al-4V

Rajesh K. Tiwari[a]; John G. Dillard
[a] Department of Chemistry, Center for Adhesive and Sealant Science, Blacksburg, VA

To cite this Article Tiwari, Rajesh K. and Dillard, John G.(2000) 'The Durability of Adhesively-bonded Ti-6Al-4V', The Journal of Adhesion, 73: 2, 233 — 258
To link to this Article: DOI: 10.1080/00218460008029308
URL: http://dx.doi.org/10.1080/00218460008029308

J. Adhesion, 2000, Vol. 73, pp. 233–258
Reprints available directly from the publisher
Photocopying permitted by license only

The Durability of Adhesively-bonded Ti-6Al-4V*

RAJESH K. TIWARI and JOHN G. DILLARD†

Department of Chemistry, Center for Adhesive and Sealant Science, Virginia Tech, Blacksburg, VA 24061-0212

(Received 19 July 1999; In final form 21 April 2000)

The durability of chromic acid-anodized Ti-6Al-4V alloy, adhesively-bonded with FM-5 supported polyimide adhesive has been studied. The performance tests compared titanium samples that had been thermally treated and bonded, and samples that were bonded and thermally treated. Following the thermal treatment, the durability was examined (1) by immersing wedge-type specimens in boiling water and measuring the crack growth and (2) by measuring the lap shear strength for single lap specimens. In the wedge tests, failure occurs within the adhesive for specimens treated at temperatures below 371°C for less than one hour. For treatments at higher temperatures and for longer periods of time, failure occurs within the anodic oxide. From the lap shear tests, the principal finding is that the lap strength decreases with increasing treatment time at constant temperature and with increasing temperature at a fixed time. For the lap specimens, failure occurs to a greater extent within the oxide as the treatment time and temperature increase. Surface analysis results indicate the formation of an aluminum fluoride species. It is reasoned that the formation of fluorine-containing materials weakens the oxide and promotes failure within the anodic oxide.

Keywords: Titanium 6Al-4V; Polyimide adhesive; Wedge specimens; Pre- and post-bonding thermal treatment; Durability; Surface analysis; Aluminum fluoride

INTRODUCTION

Titanium alloys are widely used in aerospace applications where exposure to extremes of temperature and stress is encountered in the

* One of a Collection of papers honoring F. James Boerio, the recipient in February, 1999 of *The Adhesion Society Award for Excellence in Adhesion Science, Sponsored by 3M.*

† Corresponding author. Tel.: 540-231-6926, Fax: 540-231-3255, e-mail: john.dillard@vt.edu

application of the materials [1 – 3]. Knowledge of thermal effects on the durability of adhesively-bonded specimens is essential for the design of surface treatments [4], the formulation of adhesives, and the development of models to describe failure processes.

Natan and Venables [2] studied the effect of high humidity and elevated temperature on the structural and morphological changes in titanium oxides. In the study, evidence was presented to demonstrate that anodic oxides on titanium were amorphous and that upon exposure to water, crystalline TiO and TiO_2 were produced. It was noted that oxide instability affected the durability of adhesively-bonded titanium specimens that had been exposed to humid environments. Clearfield *et al.* [5] have investigated the adhesive characteristics of oxides on titanium. A general finding was that adherends containing an anodic oxide failed within the oxide following treatment at or above 330°C in air or in vacuum. By comparison, a bonded anodized oxide on titanium specimen failed within the adhesive. In a subsequent study, Clearfield *et al.* [1] indicated that the mechanism for failure within the oxide at high temperatures was dissociation of the oxide with the formation of a non-stoichiometric oxide, and embrittlement in the alloy. Filbey and Wightman [6, 7] evaluated the durability of bonded titanium in hot-wet environments. Their principal findings were that the interpretation of results using different adhesion tests allowed different conclusions to be drawn as to the durability of adhesively-bonded systems. From a comparison of the durability of similarly-bonded titanium samples with different surface treatments, it was emphasized that interfacial properties must be included in any descriptive or predictive models for durability.

It was the objective of this investigation to conduct a systematic study of the durability of thermally-treated and bonded specimens and of bonded and thermally-treated specimens as a function of the time of thermal treatment and exposure to moisture. It was of interest to determine the extent to which a thermal pretreatment would alter the surface chemistry and to investigate the effect of surface chemical changes on durability. In the attempt to understand better the influence of the mode of stress applied to a specimen in a durability test, a comparison of the durability as a function of the test employed was also investigated.

EXPERIMENTAL

Titanium-6Al-4V samples were obtained from President Titanium, Hanover, MA. The titanium-6Al-4V plates ($10 \times 2.5 \times 0.25$ cm) were anodized in chromic acid [4] at 5 V and 13.5 amps/m^2 (1.25 amps/ft^2) for 20 min. Anodized titanium alloy was either thermally-treated and then bonded with FM-5 adhesive (heat/bond) or it was bonded and then thermally-treated (bond/heat). The adherends were not primed and were bonded with FM-5, a supported (glass cloth) polyimide (LaRC PETI-5 based) adhesive film provided by Cytec. The adhesive bond line thickness was 250 microns (0.010 in.). The adhesive specimens were cured by heating to 250°C for 30 min without pressure and then were heated to 350°C for 1 hour while a pressure of 75 psi (0.52 MPa) was applied to the specimen. The samples were cooled under pressure to room temperature at a rate of approximately 10°C/min.

The heat/bond specimens were prepared by heating the CAA-Ti alloy at 371°C for selected times in air in a furnace. The specimens were then bonded in a wedge configuration. The durability tests were carried out by immersing the bonded samples in boiling water and measuring crack length as a function of exposure time. At least four specimens were studied in each test.

For tests involving bond/heat specimens, CAA titanium-alloy specimens were bonded in wedge and single-lap shear configurations using FM-5 adhesive. The bonded samples were thermally treated at various temperatures in air for selected times. In the durability tests, wedge specimens were immersed in boiling water and crack length was measured as a function of time. For the lap shear samples, the specimens were heated in air at selected temperatures for various times, and then the specimens were tested in an Instron in air at room temperature to measure the failure force. For each test condition, four specimens were tested.

XPS spectra were obtained using a PHI Perkin-Elmer Model 5400 photoelectron spectrometer. Photoelectrons, generated using Mg K_α radiation ($h\nu = 1253.6$ eV), were analyzed in a hemispherical analyzer and detected using a position-sensitive detector. The binding energy scale was calibrated using the carbon 1s photopeak at 285.0 eV for background carbon [8]. In the presentation of the elemental results,

photoelectron spectral peak areas were measured and subsequently scaled to account for ionization probability and an instrumental sensitivity factor to yield results which are indicative of surface concentration in atomic percent. The precision and accuracy for the concentration evaluations are about 10% and 15%, respectively. Multi-component photopeaks were curve fit and the curve-fitting parameters were obtained by measuring spectra for standard materials including aluminum oxides and aluminum fluoride.

Scanning electron photomicrographs were produced using an ISI model SX-40 scanning electron microscope (SEM). Samples were sputter-coated with a thin gold film (200 Å) to reduce charging.

RESULTS

Wedge Type Specimens

The crack length results for chromic acid-anodized titanium samples that had been thermally treated and then bonded (heat/bond) are shown in Figure 1. The crack length results for an as-bonded (no thermal treatment) chromic acid anodized specimen are also given in Figure 1. The crack growth behavior for specimens that had been bonded and thermally treated (bond/heat) at 371°C for selected times are shown in Figure 2. The crack growth curves indicate no difference in performance after 5000 hours of immersion in boiling water when comparing the results for heat/bond with bond/heat specimens. It is noteworthy that the specimens that were bonded and then heated at 371°C for 3 hours failed upon insertion of the wedge. In Figure 2 a single data point is located at zero time and about 92 mm to represent this behavior. After about 150 hours of exposure in boiling water, specimens representing each treatment were removed from the test vessel, fractured, and the failure surfaces were analyzed using SEM and XPS.

The SEM photomicrographs of failure surfaces from the wedge specimens are shown in Figure 3. The SEMs in Figures 3a and 3b show the two different sides of the same sample. Since failure occurred (visual inspection) within the adhesive, it is not possible to designate the respective failure surfaces as "adherend" or "adhesive". The

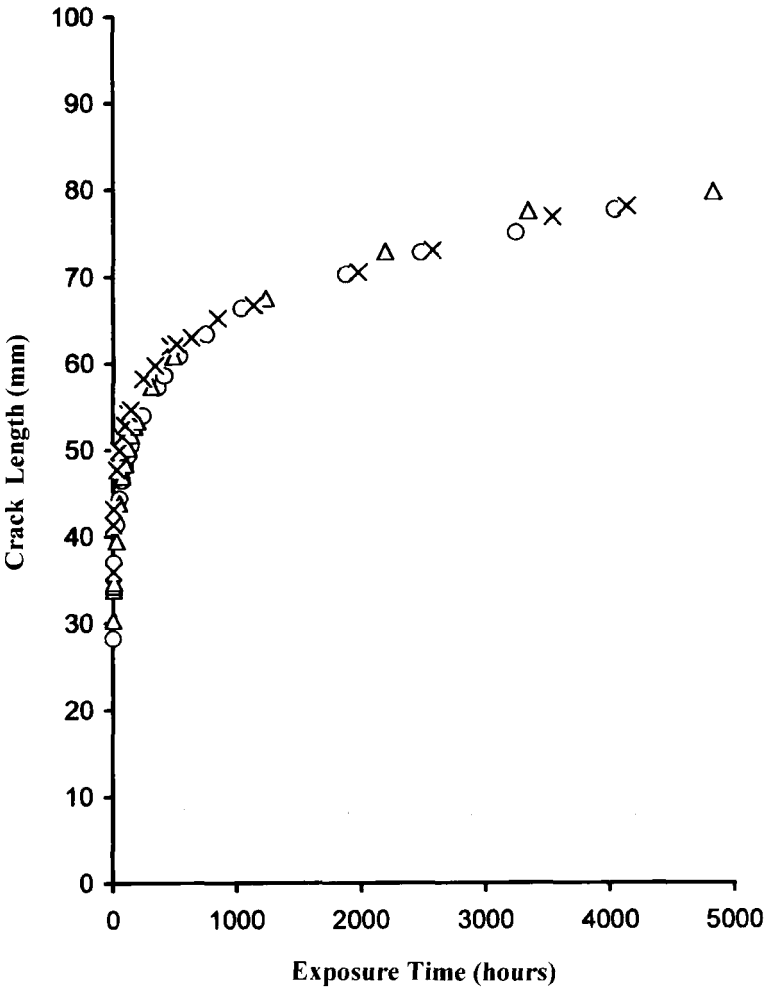

FIGURE 1 Wedge test crack length *vs.* exposure time in boiling water for non-thermally-treated CAA Ti-alloy (o) and for CAA Ti-alloy thermally-treated at 371°C for 1.0 hr (Δ), and 3 hrs (X) in air and then bonded.

surfaces are labeled arbitrarily as "A" and "B". The weave-type features in the SEM photomicrographs (Figs. 3a and 3b) are characteristic of the pattern of the woven glass scrim cloth in the adhesive. That this pattern is observed on each failure surface indicates that failure occurred within the adhesive for specimens that were

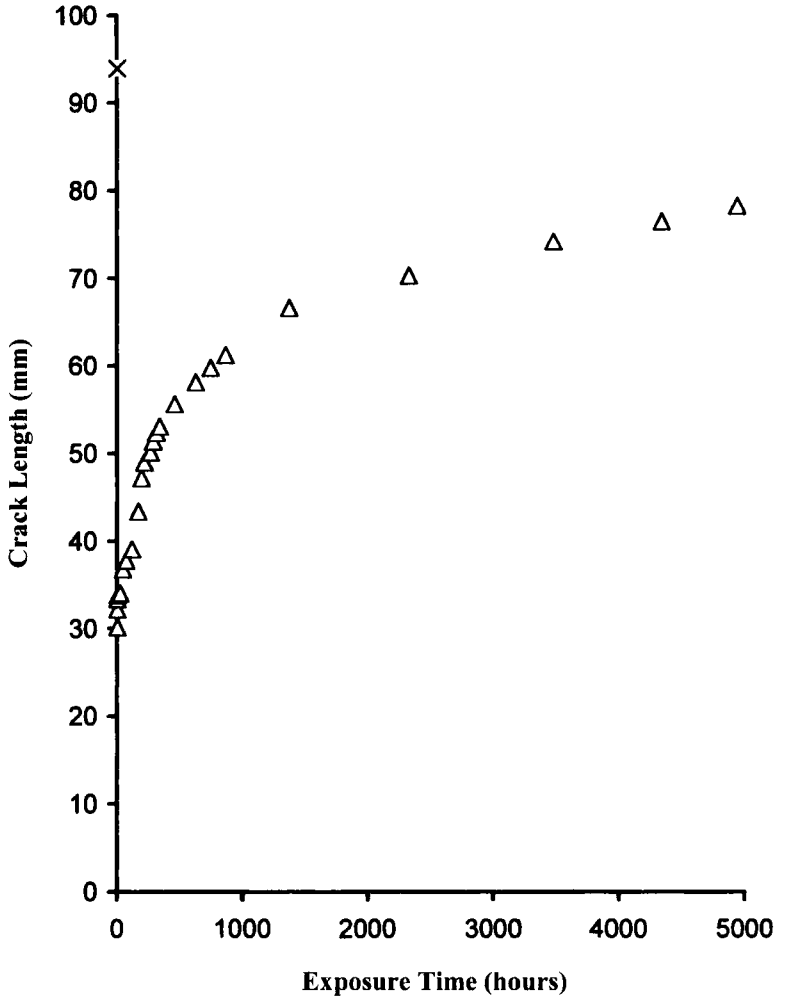

FIGURE 2 Wedge test crack length *vs.* exposure time in boiling water for CAA Ti-alloy bonded and thermally-treated at 371°C for 1.0 hr (Δ), and 3 hrs (X) in air.

prepared by a thermal treatment at 371°C for 3 hours, bonded (heat/bond) and then immersed in boiling water. For specimens that were bonded and then thermally treated at 371°C for 3 hours (bond/heat), the SEM photomicrographs (Figs. 3c and 3d) show the imprint of the adhesive, but failure is primarily within the oxide (as suggested by XPS results to be discussed in the following section). A thin layer of oxide

covers the adhesive on the surface shown in Figure 3c and the imprint of the scrim cloth is evident in Figure 3d.

The relevant XPS results for failure surfaces for heat/bond and for bond/heat specimens are summarized in Table I. The XPS results support the SEM findings and illustrate the differences in the failure modes when comparing the results for heat/bond specimens with data for bond/heat samples. In a failure that is cohesive in the adhesive, the two sides are equivalent and can be arbitrarily assigned A and B. In a failure that is in the oxide, the side that has an oxide coating on top of adhesive film is indicated as side A. The other failure side that has a very thin coating of oxide on the surface is designated as side B.

The XPS results for failure surfaces are presented for as-bonded specimens (no heat treatment) and for specimens that were heated at 371°C for 3 hrs. and then bonded, and for samples bonded and heated

FIGURE 3 SEM photomicrographs of failure surfaces from wedge test specimens: (a) and (b) are side-A and side-B of the failure surfaces of samples that were thermally treated at 371°C for 3 hrs in air and then bonded; (c) and (d) are side-A and side-B of the failure surfaces of specimens that were bonded and thermally-treated at 371°C for 3 hrs in air.

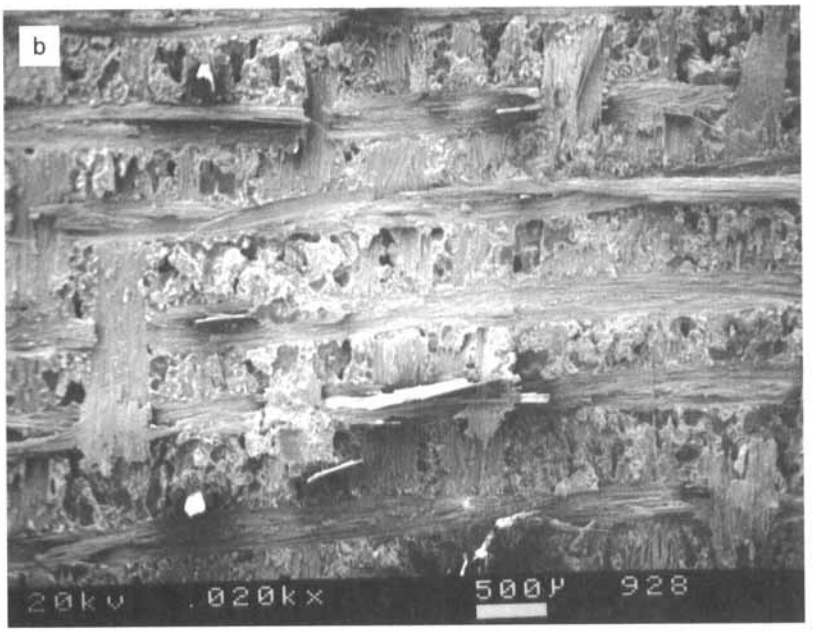

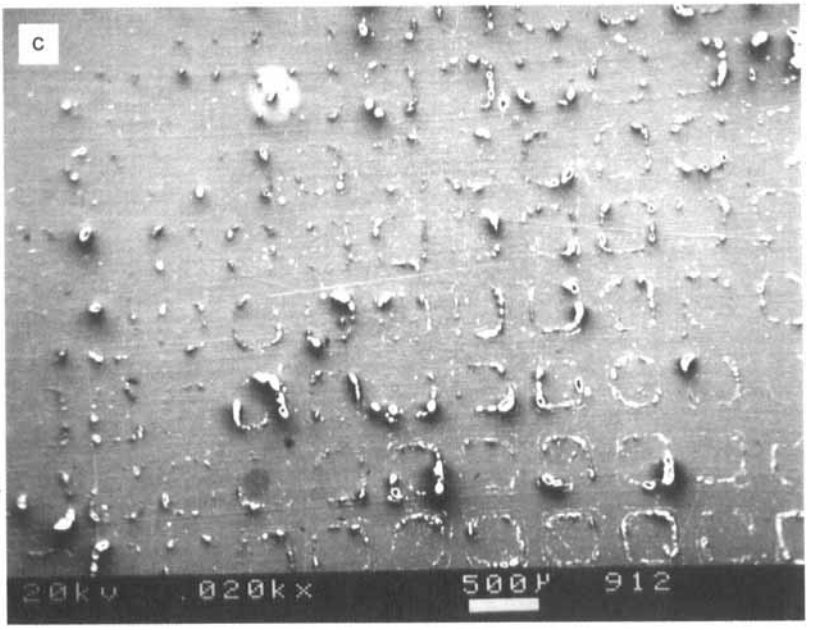

FIGURE 3 (Continued).

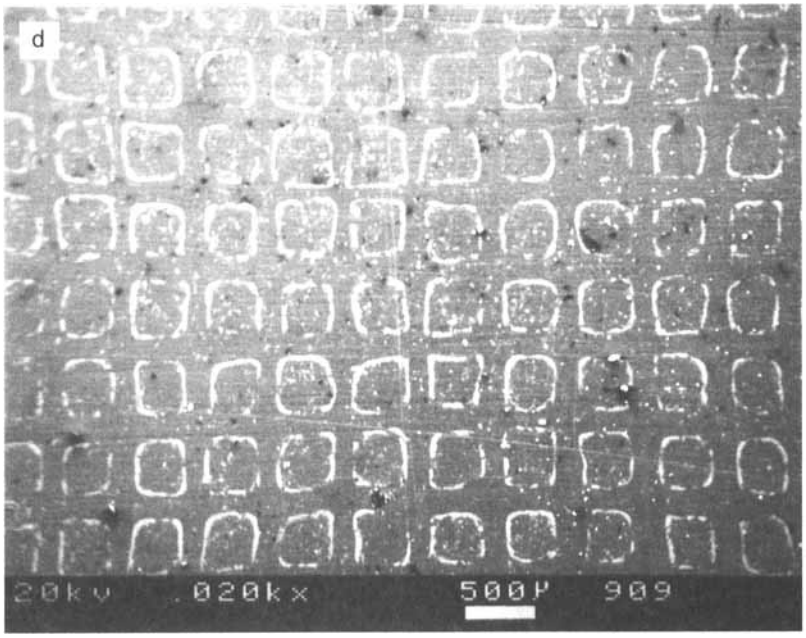

FIGURE 3 (Continued).

TABLE I XPS results for CAA Ti-6Al-4V wedge specimens thermally treated and tested in boiling water (atomic %). (Two different failure surfaces were analyzed; arbitrarily labeled A and B.)

	No treatment		*Heat and bond* 371°C/3 *hrs*		*Bond and heat* 371°C/1 *hr*		*Bond and heat** 371°C/3 *hrs*	
Element	*A*	*B*	*A*	*B*	*A*	*B*	*A*	*B*
C	73.9	73.5	74.0	73.1	71.7	73.6	17.2	33.9
O	19.1	19.5	18.2	18.6	20.4	18.2	38.5	44.0
N	4.0	3.6	4.7	5.0	4.1	3.7	1.0	0.8
Si	2.1	2.3	2.1	2.3	3.1	2.7	< 0.2	< 0.2
Ti	< 0.2	< 0.2	< 0.2	< 0.2	< 0.2	< 0.2	14.0	15.8
Al	0.9	1.1	0.6	0.6	< 0.2	1.0	7.1	2.8
F	< 0.2	< 0.2	< 0.2	< 0.2	< 0.2	< 0.2	22.2	2.7
Ca	< 0.2	< 0.2	0.4	0.4	0.7	0.8	< 0.2	< 0.2

*These specimens were not tested in boiling deionized water, because the specimens failed immediately upon insertion of the wedge.

at 371°C for 1 hr. The XPS results are similar for the analysis of each failure surface (two different surfaces from each specimen). The surface analysis results indicate that failure occurred within the

adhesive. This conclusion is supported by the fact that no titanium is detected on either failure surface for samples prepared using either treatment. Further, silicon from the scrim cloth is also detected on each failure surface at a level that is typical of that noted for specimens that fail at the scrim cloth-adhesive interface. In addition, the shape of the carbon 1s photopeak is indicative of polyimide adhesive. The XPS results demonstrate that failure occurred at the scrim cloth-adhesive interface.

Surface analysis results are also given in Table I for a specimen that was bonded and then thermally treated at 371°C for 3 hrs. The important results are that significant concentrations of titanium are detected on each failure surface, fluorine and aluminum are noted, nitrogen is at a low concentration, and silicon is not detected. It is also observed that the concentrations of aluminum and fluorine are greater on side A than on side B. That equivalent concentrations of titanium, little nitrogen, and no silicon are detected on each failure surface, indicates failure within the anodic oxide layer. The significant relative amounts of fluorine and aluminum on failure surface A suggest that these elements, or compounds containing these elements, are associated with the anodic oxide degradation process and contribute to failure in the durability tests.

The curve fit XPS spectra in the aluminum 2p and fluorine 1s regions for an as-anodized titanium alloy surface and for the "A" side surface of the failed bond/heat sample (371°C for 3 hrs) are presented in Figure 4. The respective Al 2p and F 1s spectra for the as anodized, non-treated specimen exhibit only one photopeak. The binding energy for aluminum suggests the presence of an aluminum oxide or hydrated oxide, while the binding energy for fluorine indicates adsorbed fluoride ion. Adsorbed fluorine arises from HF that is added to the anodizing solution to control current density. From an XPS depth profile analysis of an as-anodized titanium-alloy sample (Tab. II), fluoride is present not only on the surface of the oxide coating but is also present within the oxide coating. The fluorine concentration increases from about 5 at.% at the surface to almost 10 at.% at a depth of 35 nm. The fluoride ion could be present as adsorbed anion [9] and/or fluoride could be located in the metal oxide lattice as a substitute for O^{2-} ions. Since F^- and O^{2-} anions have very similar ionic radii [10], the substitution of O^{2-} anions by fluoride ions in metal oxides is common

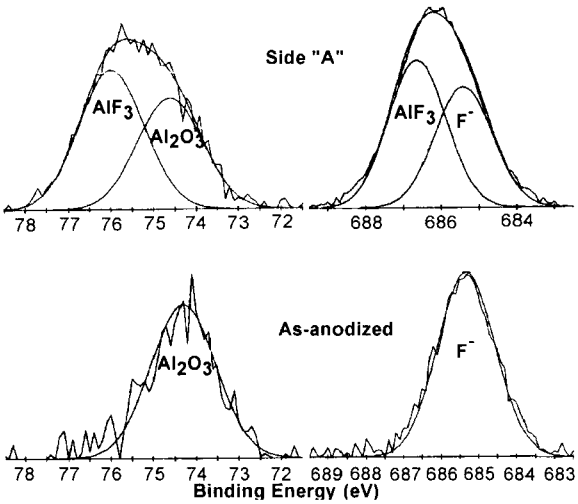

FIGURE 4 Curve-fit XPS analysis of fluorine 1s and aluminum 2p photopeaks for (a) A side failure surface for a specimen bonded and thermally-treated at 371°C for 3.0 hr in air and (b) an as-CAA-anodized Ti-6Al-4V alloy surface.

TABLE II XPS depth profile results for a CAA Ti-6Al-4V (as anodized) adherend (atomic %)

Element	*Surface*	*5 nm*	*15 nm*	*25 nm*	*35 nm*
C	22.8	15.3	13.4	12.6	9.1
O	50.9	50.7	50.8	50.6	51.3
Ti	18.4	21.2	23.2	23.6	25.7
Al	3.0	4.0	3.8	3.9	4.2
F	4.9	8.8	8.8	9.2	9.6

[11, 12]. Fluoride could also be associated with hydrogen in the form of hydrofluoric acid, since metal oxides in general retain some amount of moisture when exposed to the atmosphere at ambient temperature. The exact chemical nature of the fluoride ion in the oxide coating of the as-anodized alloy has not been studied in detail.

The aluminum 2p and the fluorine 1s photopeaks from XPS analysis of failure surfaces (side A) for bond/heat samples from wedge tests could each be resolved into two components. Each new component occurs at a binding energy that is higher than that for aluminum oxide or adsorbed fluorine. The binding energies for aluminum and fluorine as fluoride from the curve fit data were 76.1 eV and 686.7 eV,

respectively. These binding energies are in close agreements with the reported values for aluminum and fluorine in AlF_3 [13, 14]. Based on binding energy data for AlF_3, the high binding energy peak for aluminum is assigned to aluminum fluoride. The high binding energy peak for fluorine is attributed to fluorine in aluminum fluoride.

Using the atomic percentages for the aluminum–fluorine components in the Al 2p and F 1s peak envelopes, an approximate empirical formula for an aluminum–fluorine compound was determined. From XPS curve-fit analysis of the "A" oxide-failure regions of bond/heat specimens, the fluorine-to-aluminum ratio ranged between 2.9 and 4.0, with an average ratio of 3.4. The ratio closely agrees with that for an aluminum fluoride (AlF_3) composition. The higher F/Al ratios (F/Al > 3.0) on some failure surfaces may be due to aluminum fluoride complexes of the form $[AlF_n^{(n-3)-}]$ in combination with some aluminum oxy-fluoride $[Al(OF)_x]$ compounds.

Fluoride ion in the anodic oxide coating of the titanium alloy could react with metal compounds to form metal fluorides. Based on the evidence obtained from XPS analysis of failure specimens, aluminum formed aluminum fluoride. One possible reaction for the formation of aluminum fluoride is given below. Aluminum oxide and hydrofluoric acid present in the CAA oxide coating could react to produce aluminum fluoride during the thermal treatment following bonding.

$$Al_2O_3(s) + 6HF(g) \rightarrow 2AlF_3(s) + 3H_2O(l)$$

ΔG^0 for the above reaction at 25°C is -343.4 kJ/mol as calculated from literature data [15, 16]. The negative ΔG^0 value for the reaction suggests that the above process is at least thermodynamically favorable at 25°C.

Based on the surface analysis results and thermodynamic considerations, it is reasoned that failure in the durability tests is due to the formation of an aluminum fluoride which destroys the integrity of the CAA anodic oxide. The degradation reaction occurs in the bonded specimens during the various "bond/heat" thermal treatments.

Lap-shear Specimens

The average lap shear strengths and the failure modes (visual inspection) for bonded and thermally-treated specimens are summarized

in Table III. The lap shear specimens that were thermally treated in air at 177°C for 4 weeks and at 204°C for 1 week exhibited the same failure strength as that for the non-thermally treated specimen. The lap-shear strength decreased to about 6500 psi (44.8 MPa) for specimens that had been thermally treated at 177°C for 4 months and at 204°C for 4 weeks. The failure mode for non-thermally treated and for the specimens treated at 177°C and 204°C was principally cohesive, within the adhesive. For these samples the scrim cloth pattern was visually evident and XPS results shown in Table IV confirmed failure in the adhesive at the scrim cloth-adhesive interface. The XPS results for the two failure surfaces are equivalent. The atomic concentrations for carbon, oxygen, nitrogen, and silicon are typical of the values obtained for failure surfaces that are produced *via* debonding within the adhesive. The elements, titanium, aluminum and fluorine were not detected on these failure surfaces.

TABLE III Lap shear strengths and failure (visual) modes for different thermal treatments. [Failure modes: C = cohesive (within the adhesive), A = adhesive (interfacial)]

Treatment conditions	*Lap strength, psi (MPa)*	*Failure mode (visual)*
No treatment	7183 (49.5)	100% C
177°C/4 weeks	7080 (48.8)	100% C
177°C/4 months	6475 (44.6)	99% C, 1% A
204°C/1 week	7279 (50.2)	100% C
204°C/4 weeks	6510 (44.9)	95% C, 5% A
350°C/0.5 hr	5776 (39.8)	100% C
350°C/1 hr	4559 (31.4)	90% C, 10% A
350°C/2 hrs	4379 (30.2)	90% C, 10 % A
350°C/3 hrs	5181 (35.7)	95% C, 5% A
350°C/5 hrs	3030 (20.9)	73% C, 27% A
350°C/11 hrs	2200 (15.2)	60% C, 40% A
350°C/24 hrs	1341 (9.3)	3% C, 97% A
371°C/0.5 hr	3646 (25.1)	92% C, 8% A
371°C/1 hr	2859 (19.7)	68% C, 32% A
371°C/2 hrs	2040 (14.1)	78% C, 22% A
371°C/3 hrs	1661 (11.5)	39% C, 71% A
385°C/0.5 hr	3148 (21.7)	82% C, 18% A
385°C/1 hr	1407 (9.7)	33% C, 67% A
385°C/2 hrs	1640 (11.3)	25% C, 75% A
385°C/3 hrs	593 (4.1)	3% C, 97% A
399°C/0.5 hr	1694 (11.7)	56% C, 44% A
399°C/1 hr	1534 (10.6)	28% C, 72% A
399°C/2 hrs	900 (6.2)	1% C, 99% A
399°C/3 hrs	462 (3.2)	100% A

TABLE IV XPS results for CAA Ti-6Al-4V lap specimens (non-thermally treated), bonded and tested in air at room temperature (atomic %). (Two different failure surfaces analyzed; arbitrarily labeled A and B.)

	Non-treat (cohesive)	
Element	*A*	*B*
C	72.9	73.5
O	18.5	18.1
N	4.9	5.1
Si	3.7	3.3
Ti	< 0.2	< 0.2
Al	< 0.3	< 0.3
F	< 0.2	< 0.2

For specimens thermally treated at 350°C, 371°C, 385°C and 399°C two distinct failure regions were noted on the failed specimens. The regions corresponded to adhesive (interfacial – at the oxide : adhesive interface) or cohesive (within the adhesive) failures. The lap-shear strengths, as well as the extent of cohesive failure, decreased with an increase in treatment time at a given temperature or with an increase in temperature at a comparable time. Irrespective of the thermal history of the sample, the XPS results for both failure surfaces in the cohesive failure region were equivalent. These "cohesive" failure surfaces contain carbon, oxygen, nitrogen, and silicon at concentration levels that are characteristic of failure within the adhesive and specifically at the adhesive-scrim cloth interface.

XPS analyses of the interfacial failure regions are given in Table V for lap shear samples that had been bonded and thermally treated at 385°C for 2 and 3 hours, respectively, and tested. The XPS results reveal significant amounts of titanium, aluminum, fluorine, and oxygen, in addition to smaller amounts of carbon, nitrogen and silicon. These data support the notion that interfacial failure occurs within the oxide layer, rather than at the interface between the adhesive and oxide coating. For each set of failure analysis results, failure surface A exhibits a greater concentration of fluorine and aluminum, while the content of oxygen is significantly greater and titanium is slightly greater on the B failure surfaces. The non-equivalent nature of the respective failure surfaces indicates that failure is promoted in a boundary region where one domain is rich in aluminum fluoride along with titanium oxide, and the other region is

TABLE V XPS results for CAA Ti-6Al-4V lap specimens thermally treated at 385°C for 2.0 and 3.0 hr in air and tested in air (atomic%). (Two different failure surfaces analyzed: arbitrarily labeled A and B.)

	Bond and heat 2.0 hr (i'facial region)		*Bond and heat 3.0 hr (i'facial region)*	
Element	*A*	*B*	*A*	*B*
C	23.7	22.4	18.5	15.3
O	39.3	50.2	39.0	54.8
N	1.4	1.3	1.5	0.9
Si	2.5	4.1	3.9	5.7
Ti	13.0	14.3	12.7	15.4
Al	4.8	3.1	5.1	2.9
F	15.3	4.6	19.3	5.0

characterized by titanium and aluminum oxides with smaller contributions from fluorine-containing components (principally with aluminum).

The binding energy of titanium suggests that titanium is present as a titanium(IV) oxide. The measured binding energies for aluminum suggest that aluminum is present not only in the oxide form but also as fluoride. The curve fit analyses for the fluorine photopeak are consistent with fluorine as an adsorbed fluoride and as fluoride in an aluminum fluoride. These findings are similar to the results discussed earlier for the analysis of failure surfaces from the wedge specimen durability tests. It was also noted that the amount of "aluminum fluoride" on the failure surfaces increased with increasing treatment temperature and duration of treatment. The presence of fluorine and an aluminum fluoride at significant concentrations on the interfacial failure surfaces suggests that the formation of an "aluminum fluoride" is associated with the degradation and debonding process for bonded lap shear specimens treated at elevated temperatures.

DISCUSSION

In a series of investigations by Clearfield *et al.* [1, 5], CAA titanium alloy was subjected to thermal treatment at 330°C for 160 and 2000 hours in air. CAA titanium alloy was also exposed to higher treatment temperatures, 400°C for 24 hrs and 450°C for 3 hr and 24 hrs, but the thermal treatment was carried out in vacuum. The locus of failure was

in the oxide for a CAA specimen that was thermally treated in vacuum at 400°C and 450°C. The CAA titanium specimen thermally treated at 330°C in air failed *via* mixed mode when treated for 160 hrs, whereas failure was in the oxide coating when treated for 2000 hours. Clearfield and co-worker observed a significant tailing of the oxygen signal (metal/oxide interface was not sharp) in AES depth profile spectra of a thermally-treated (in vacuum) CAA Ti-6Al-4V alloy. The oxygen concentration immediately below the surface was near the solubility limit (about 25 at.%) in the alloy. Clearfield and associates suggested that at temperatures approaching 300°C oxide dissolution takes place. The dissolution of oxygen results in non-stoichiometric oxides and an embrittled region below the oxide. These regions could weaken the oxide of the interphase and cause bond failure.

In the current work, the high-temperature studies were carried out in the temperature range 350°C to 399°C, for a much shorter time, 0.5 hour to 3 hours (24 hours only at 350°C), in air. At this treatment temperature and experimental time scale, the extent of oxygen dissolution into the metal is not large enough to cause any significant decrease in the oxide strength. The Auger sputter-depth profiles for as anodized CAA Ti-6Al-4V alloy and CAA Ti-6Al-4V alloy thermally treated at 371°C for 3 hrs in air are shown in Figure 5. There is no significant difference in the two Auger depth profiles, except for an

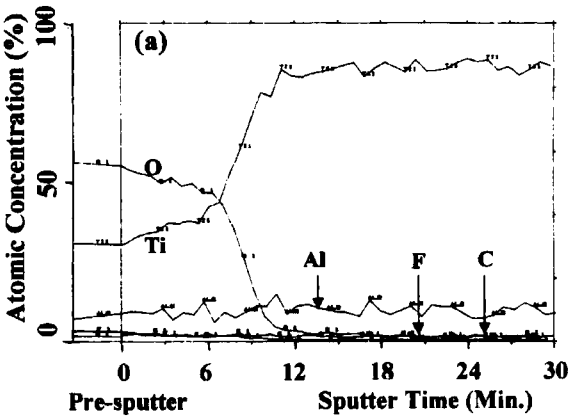

FIGURE 5 Auger sputter-depth profile of (a) as-anodized CAA Ti-6Al-4V alloy and (b) CAA Ti-6Al-4V alloy thermally-treated at 371°C for 3.0 hrs in air.

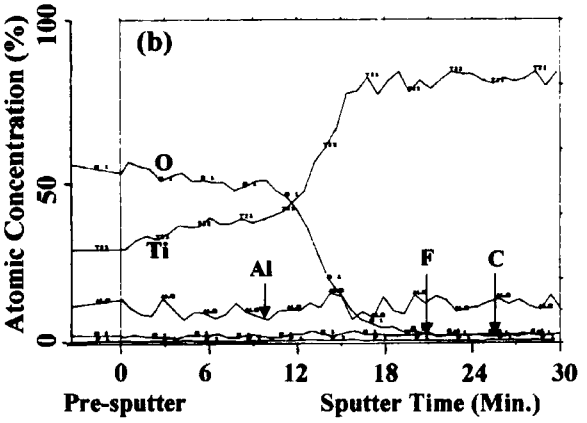

FIGURE 5 (Continued).

increase in the oxide thickness for the thermally-treated specimen due to thermal oxidation. The metal/oxide interface is sharp and no significant tail of the oxygen signal is observed for thermally-treated CAA Ti-6Al-4V alloy.

In the wedge specimens, it could be anticipated that oxygen dissolution would be dissimilar in a non-bonded CAA titanium alloy compared with a bonded specimen since the CAA titanium alloy surface in the former is comparatively less protected from the oxidizing environment. If oxygen dissolution plays a significant role in causing bonds to fail at the oxide/metal interface, then the heat/bond wedge specimen should have failed in the oxide coatings. XPS results for thermally-treated (371°C for 3.0 hours) wedge specimens indicate bond failure in the adhesive for the heat/bond specimen and in the oxide for the bond/heat specimen. It does not appear that this difference in the failure modes for heat/bond and bond/heat specimens could be explained on the basis of an oxygen-dissolution mechanism.

The XPS and AES characterization results suggest that failure takes place within the anodic oxide coating, mostly near the oxide/metal interface. The XPS results of the interfacial failure region reveal significant amounts of titanium, aluminum, fluorine and oxygen, in addition to smaller amounts of carbon, nitrogen and silicon. The presence of adhesive as well as fluorine in the oxide coating on both

failure surfaces suggests that the locus of failure is not at the oxide/metal interface. Recall that one failure surface (side A) has relatively larger amounts of aluminum and fluorine compared with the other failure surface, side B. Side A has a relatively thicker oxide coating on top of the adhesive film and side B has a very thin oxide coating (5–10 nm). The AES sputter depth profile results (atomic concentration *versus* sputter time) of failure surfaces of the bond/heat (371°C/3 hrs/air)-wedge specimen are shown in Figure 6. Since a metal surface is easily oxidized upon exposure to air, a thin oxide layer on the metal side (side B) of the failure surface may indicate bond failure at the metal/oxide interface. The fact that the XPS surface analysis reveals

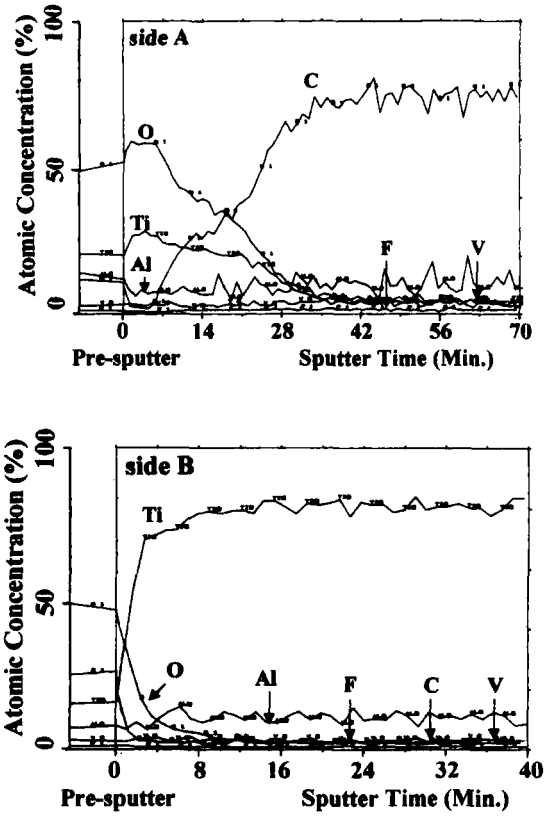

FIGURE 6 AES sputter-depth profiles for the failure surfaces of bond/heat (371°C/3.0 hrs/air)-wedge specimen: (a) side A and (b) side B.

fluorine (one of the chemical constituents of the CAA oxide coating) on side B indicates that failure is definitely in the anodic oxide coating. The AES sputter depth profile of side A indicates a relatively thick oxide coating on the adhesive film. However, the oxide/adhesive interface is not sharp. The presence of carbon in the oxide layer indicates good wetting of the porous oxide by the adhesive film during the bonding process. A schematic diagram, showing the cross-sectional side view of the metal/oxide/adhesive interface and the locus of failure in the oxide coating, is shown in Figure 7.

A number of reasons for the weakening of the oxide film could be suggested, but three possibilities merit discussion. (1) The formation of aluminum fluoride species, as a result of reaction between hydrofluoric acid and aluminum oxide, introduces large compressive stresses in the oxide due to an increase in the oxide volume. The densities of titanium oxide (TiO_2), aluminum oxide (Al_2O_3) and aluminum fluoride (AlF_3) are 4.24 g/cm^3, 3.965 g/cm^3 and 2.882 g/cm^3, respectively [17, 18]. The

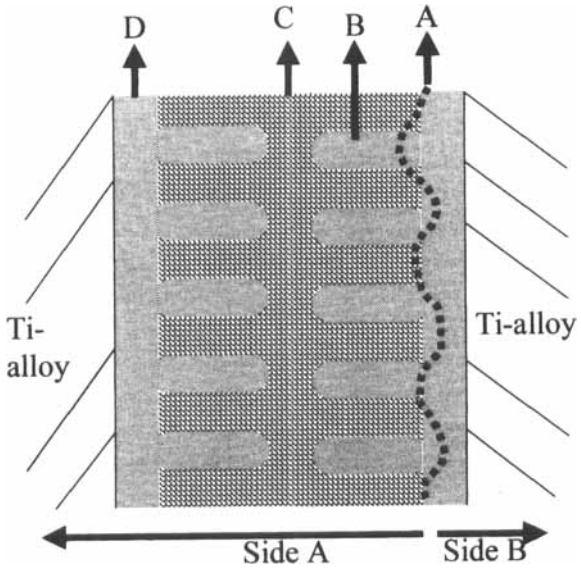

FIGURE 7 Schematic diagram showing the cross-sectional side view of the metal oxide/adhesive interface and the locus of failure in the oxide coating, where A (dotted line) represents the locus of failure, B is the anodic oxide column, C is the adhesive, and D is the barrier oxide layer.

presence of compressive stresses in the oxide could result in cracking and spalling of the oxide coating under minimal load (mechanically weak oxide film). (2) The fluoride ions could directly react with the metal at the oxide/metal interface to form products at the interface, which could lead to the weakening or even debonding of the oxide from the metal (*e.g.*, $2Al + 6HF = 2AlF_3 + 3H_2$). (3) Any significant differences in the coefficients of thermal expansion (CTE) between oxides and fluorides could result in a stress built-up inside the oxide when the test sample is cooled after the thermal treatment. Such stresses could promote failure in the oxide.

The difference in the failure mode when comparing the bond/heat and heat/bond is attributed to the formation of an aluminum fluoride. The basic difference between the two treatments, heat/bond and bond/heat, is in the chemical composition of their respective anodic oxide coatings. Fluorine is not detected in the CAA oxide coatings when a CAA Ti-6Al-4V alloy (non-bonded) is thermally treated at 371°C for 3.0 hours in air. The wide scan XPS spectra of a CAA Ti-6Al-4V alloy with and without thermal treatment are shown in Figure 8. The XPS photopeak at 685 eV corresponding to adsorbed fluoride ion is absent in the thermally-treated CAA titanium alloy. The XPS depth profile results for CAA titanium alloy thermally treated at 371°C for 3.0 hours in air are summarized in Table VI. The XPS depth profile data clearly show the absence of fluorine in the anodic oxide coatings. A plausible explanation is that a fluorine-containing compound, perhaps HF, in the oxide coating is removed *via* desorption. On the other hand, when CAA titanium alloy is bonded prior to any thermal treatment, fluoride ions are trapped within the oxide coating due to wetting of the oxide by the adhesive film during the bonding process. Thus, when a CAA titanium alloy is bonded and then thermally treated at high temperatures (> 350°C), the fluoride ions in the oxide coating react with aluminum to form aluminum fluoride species.

Although the reaction between aluminum oxide and hydrofluoric acid is thermodynamically favorable at room temperature, the reaction does not take place at any noticeable rate at room temperature. Therefore, it is not surprising that the industrial production of aluminum fluoride is carried out by a dry process, where Al_2O_3 is treated at 550°C to 600°C in a continuous stream of gaseous hydrofluoric acid [19].

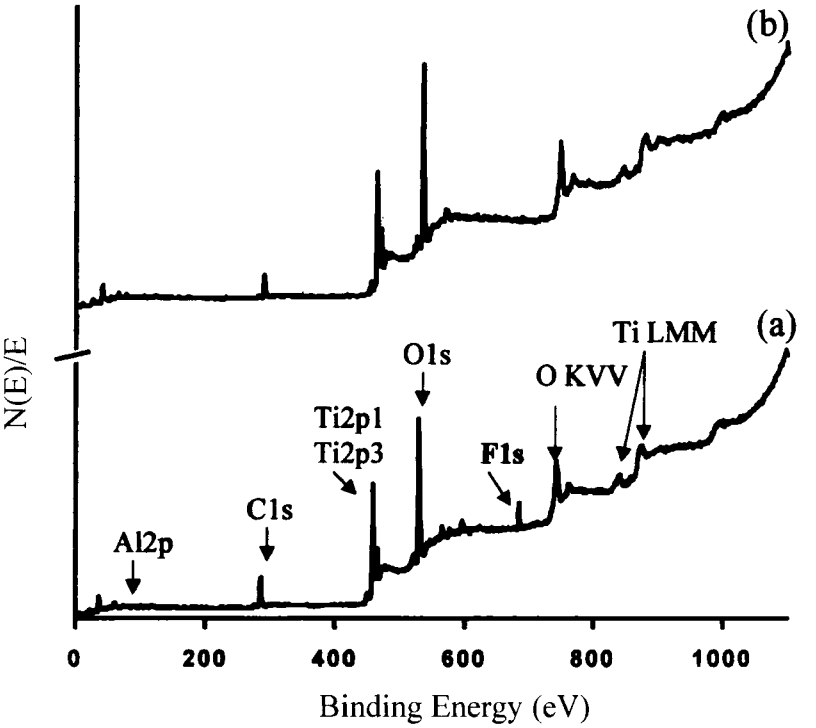

FIGURE 8 XPS wide scan spectra for (a) as-anodized CAA Ti-6Al-4V alloy and (b) CAA Ti-6Al-4V alloy thermally-treated at 371°C for 3.0 hrs in air.

TABLE VI XPS depth profile results for CAA Ti-6Al-4V adherend, thermally treated at 371°C for 3.0 hours in air (atomic%)

Element	*Surface*	*5 nm*	*15 nm*	*25 nm*	*35 nm*
C	24.8	14.8	10.1	9.7	8.5
O	53.8	58.5	58.4	57.8	57.7
Ti	17.3	22.2	26.9	27.7	28.8
Al	4.1	4.5	4.6	4.8	5.0
F	< 0.2	< 0.2	< 0.2	< 0.2	< 0.2

On the other hand, the absence of fluoride ions in the oxide coatings for a heat/bond specimen does not facilitate the formation of aluminum fluoride species and, thus, there is no weakening of the anodic oxide coatings. However, it must also be pointed out that the bond/heat wedge specimen that is thermally treated at 371°C for 1.0

hour in air does not fail in the oxide coating. The absence of failure in the oxide could be due to the fact that an insufficient quantity of aluminum fluoride has formed to cause oxide failure under the given mechanical load (wedge) condition. It is known from single-lap test results (See Tab. III) that thermally-treated lap specimens increasingly fail in the oxide coating as the temperature and duration of thermal treatment are increased.

In this study, the temperature at which fluorine is completely desorbed from the oxide coating has not been determined. But, XPS studies involving CAA titanium alloy thermally treated at 200°C for 1 hour in air indicate that fluorine is still present in the oxide coating in significant amounts (1.4 at.% and 3.8 at.% on the surface and at 35 nm depth, respectively). The presence of fluoride ions in the metal oxide lattice suggests that higher treatment temperatures would be required to remove fluorine completely from the oxide coating.

In the thermal treatment studies, it was reasoned that the formation of aluminum fluoride species weakens the oxide and promotes failure within the anodic oxide coatings. Therefore, it is meaningful to follow the reaction kinetics for the formation of aluminum fluoride species. The binding energies of fluorine and aluminum are different as aluminum fluorides from what they would be as absorbed ions and oxide, respectively. Therefore, fluorine and/or aluminum with their characteristic binding energies in aluminum fluorides can be used as fingerprints to follow the reaction kinetics of aluminum fluoride. By plotting concentration of fluorine or aluminum as fluorides *versus* thermal treatment time at various temperatures, the rate of aluminum fluoride formation is obtained at respective temperatures. The activation energy (E_a) for the formation of aluminum fluoride species is then determined from the slope of the Arrhenius plot (log (reaction rate) *vs.* $1/T$).

The average concentration of fluorine, as aluminum fluoride, on the failure surfaces of thermally-treated lap specimens is determined from XPS curve-fit analysis of the fluorine photopeak. Similarly, the average concentration of aluminum, as aluminum fluoride, on the failure surfaces of thermally-treated lap specimens is determined from the XPS curve-fit analysis of the aluminum photopeak. XPS test results from only side A of the failure surfaces were used for the purpose of studying aluminum fluoride reaction kinetics. The reaction

rate data for the formation of aluminum fluoride species using fluorine as fingerprint element are shown in Figure 9. With just four data points at each temperature, it is difficult to determine, with a good degree of confidence, the rate law for the reaction. However, data for the formation of aluminum fluoride species fitted reasonably well ($R^2 = 90$) a linear reaction rate equation of the form $y = kt + c$, where y is the concentration of fluorine or aluminum as aluminum fluoride; k is the reaction rate constant; t is the elapsed time of the reaction (thermal treatment time); and c is a constant. The linear reaction rate constants, as determined from linear plots of aluminum and fluorine kinetics data at various temperatures, are listed in Table VII. The rate of aluminum fluoride formation as a function of treatment temperature in the form of an Arrhenius plot is shown in Figure 10.

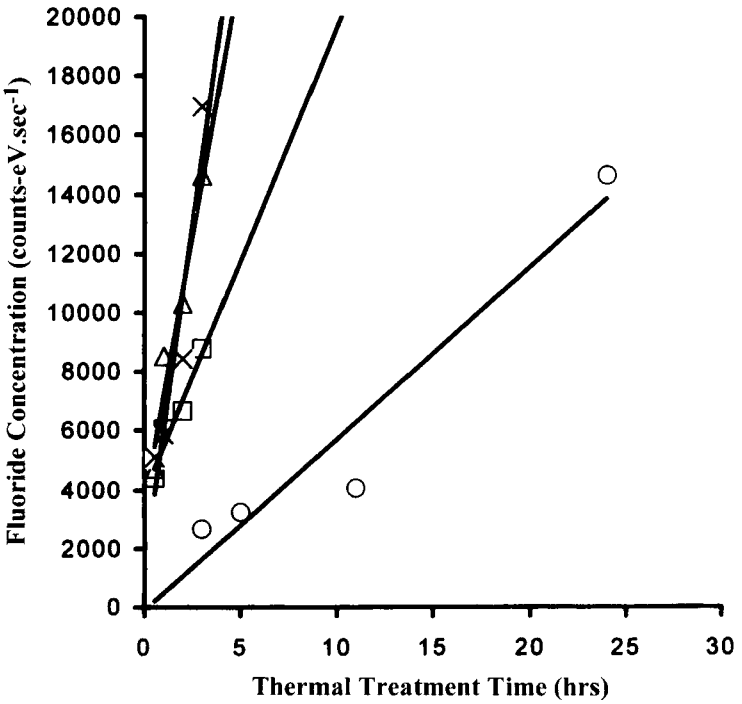

FIGURE 9 Concentration of fluorine, as fluoride, plotted *vs.* the thermal treatment time at various treatment temperatures: (o) 350°C, (□) 371°C, (Δ) 385°C and (X) 399°C; straight lines are the least-squares fits from the regression analyses.

TABLE VII Linear rate constants for the aluminum–fluorine reaction

Temperature(°C)	*Fluorine* (*cts-ev/sec-hr*)	*Aluminum* (*cts-ev/sec-hr*)
350	580	170
371	1570	600
385	3630	1060
399	4640	1160

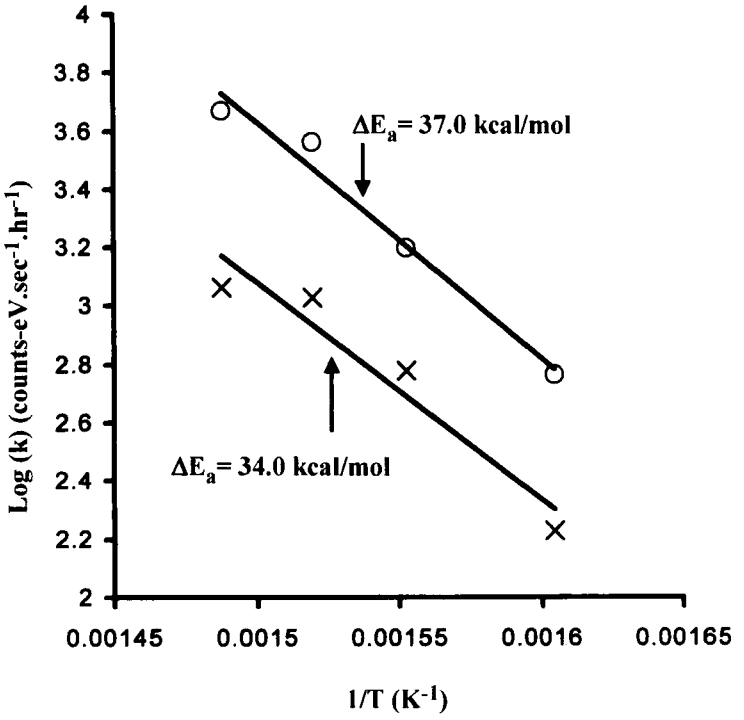

FIGURE 10 Arrhenius plot: rate of aluminum fluoride formation *vs.* $1/T$: (o) linear rate constants from fluorine kinetic data; (X) linear rate constants from aluminum kinetic data; straight lines are the least-squares fits from the regression analyses.

The activation energy values obtained from Arrhenius plots using aluminum and fluorine kinetic data are about the same. The average activation energy for the formation of aluminum fluoride species is approximately 36 kcal/mole. The high activation energy suggests that the rate of aluminum fluoride formation is substantial only at high temperatures.

SUMMARY AND CONCLUSIONS

Chromic acid anodized and bonded titanium 6-Al-4V specimens are degraded by high-temperature thermal treatments. Crack propagation for wedge specimens immersed in boiling water is equivalent for samples having had no thermal treatment and for those treated at elevated temperatures for less than three hours. However, the mode of failure changes from cohesive (within the adhesive at the scrim cloth-adhesive interface) to interfacial (within the anodic oxide) as either the temperature or time of treatment is increased. The lap-shear failure strength decreases and the failure mode changes from predominantly cohesive failure (at the adhesive-scrim cloth interface) to interfacial as the time of thermal treatment is increased. It is argued that failure is promoted by the formation of an "aluminum fluoride" that results from a reaction of residual fluorine from the anodizing bath and aluminum in the alloy.

Acknowledgments

Thanks are expressed to the NASA Langley Research Center, to the Boeing Commercial Airplane Company, to the NSF-STC at Virginia Tech (National Science Foundation Grant DMR-9120004), and to the Commonwealth of Virginia for financial support. It is essential to thank Frank Cromer in the Virginia Tech Surface Lab for his continued excellent work.

References

[1] Clearfield, H. M., Shaffer, D. K., Vandoren, S. L. and Ahearn, J. S., *J. Adhesion* **29**, 81 (1989).
[2] Natan, M. and Venables, J. D., *J. Adhesion* **15**, 125 (1983).
[3] Davis, G. D., *Surf. Iface. Anal.* **17**, 439 (1991).
[4] Clearfield, H. M., McNamara, D. K. and Davis, G. D., "Surface Preparation of Metals", In: *Engineered Materials Handbook. Adhesives and Sealants*, Vol. 3, Brinson, H. F. Ed. (ASM International, Materials Park, OH, 1990), p. 259.
[5] Clearfield, H. M., Shaffer, D. K., Ahearn, J. S. and Venables, J. D., *J. Adhesion* **23**, 83 (1987).
[6] Filbey, J. A. and Wightman, J. P., *J. Adhesion* **28**, 1 (1989).
[7] Filbey, J. A. and Wightman, J. P., "Factors Affecting Durability of Titanium/Epoxy Bonds", In: *Adhesion 12*, Allen, K. W. Ed. (Elsevier, New York, 1988), p. 17.

[8] Briggs, D., "Applications of XPS in Polymer Technology", In: *Practical Surface Analysis by Auger and X-Ray Photoelectron Spectroscopy*, Briggs, D. and Seah, M. P. Eds. (John Wiley, New York, 1983), p. 359.
[9] Sanchez, J. and Augustynski, J., *J. Electronal. Chem.* **103**, 423 (1979).
[10] Shannon, R. D. and Prewitt, C. T., *Acta Crystallogr. Sect. B* **B25**, 925 (1968).
[11] *Inorganic Solid Fluorides Chemistry and Physics*, Hagenmuller, P. Ed. (Academic Press, Inc., London, 1985), p. 5.
[12] Kirklin, P. W., Auzins, P. and Wertz, J. E., *J. Phys. Chem. Solids* **26**, 1067 (1965).
[13] McGuire, G. E., Schweitzer, G. K. and Carlson, T. A., *Inorg. Chem.* **12**, 2451 (1973).
[14] Wang, Y. A., Miura, Y. and Tsugaru, T., *J. Mater. Sci. Lett.* **8**, 421 (1989).
[15] Chase, M. W. Jr., Davies, C. A., Downey, J. R. Jr., Frurip, D. J., McDonald, R. A. and Syverud, A. N. Eds., *JANAF Thermochemical Tables*, 3rd edn. (American Chemical Society, Washington D. C., 1986).
[16] Atkins, P. W., *Physical Chemistry*, 3rd edn. (ELBS Oxford University Press, 1986), p. 117.
[17] Miyayama, M., Koumoto, K. and Yanagida, H., "Engineering Properties of Single Oxides, In: *Engineered Materials Handbook*, Vol. 4: Ceramics and Glasses; Schneider, S. J., Tech. Chair. (ASM International: USA, 1991), p. 748.
[18] *Handbook of Chemistry and Physics*, Lide David, R. Ed. (CRC Press, Boca Raton, FL, USA), 72nd edition, 1991–92, p. 4.
[19] *Inorganic Solid Fluorides Chemistry and Physics*, Hagenmuller, P. Ed. (Academic Press, Inc., London, 1985), p. 579.